Supporting Information for

Synthesis and excited state processes of arrays containing amine-rich carbon dots and unsymmetrical rylene diimides

Luka Đorđević,[a,†,‡,*] Philipp Haines,[b] Michele Cacioppo,[a] Francesca Arcudi,[a‡] Tobias Scharl,[b] Alejandro Cadranel,[b,c,d] Dirk M. Guldi,[b,*] and Maurizio Prato[a,e,f,*]

[a.] *Department of Chemical and Pharmaceutical Sciences, University of Trieste, and INSTM UdR Trieste, Via Licio Giorgieri 1, 34127 Trieste, Italy.*

[b.] *Department of Chemistry and Pharmacy, Interdisciplinary Center for Molecular Materials, Friedrich-Alexander Universität Erlangen-Nürnberg, Egerlandstraße 3, 91058 Erlangen, Germany.*

[c.] *Universidad de Buenos Aires, Facultad de Ciencias Exactas y Naturales, Departamento de Química Inorgánica, Analítica y Química Física, Pabellón 2, Ciudad Universitaria, C1428EHA, Buenos Aires, Argentina.*

[d.] *CONICET – Universidad de Buenos Aires. Instituto de Química Física de Materiales, Medio Ambiente y Energía (INQUIMAE), Pabellón 2, Ciudad Universitaria, C1428EHA, Buenos Aires, Argentina.*

[e.] *Center for Cooperative Research in Biomaterials (CIC biomaGUNE), Basque Research and Technology Alliance (BRTA), Paseo de Miramon 182, 20014, Donostia San Sebastián, Spain.*

[f.] *Basque Foundation for Science, Ikerbasque, Bilbao 48013, Spain.*

† Present address: Simpson Querrey Institute, Northwestern University, 303 E. Superior, Chicago, Illinois 60611, United States.

‡ Present address: Department of Chemistry, Northwestern University, 2145 Sheridan Road, Evanston, Illinois 60208, United States.

Table of Contents

1. Instruments and Materials

Thin layer chromatography (TLC) was conducted on pre-coated aluminum sheets with 0.20 mm Merck Silica Gel F254.

Column chromatography was carried out using Merck silica gel 60 Å (particle size 40-63 µm or 60-200 µm). Gel filtration chromatography was performed with Sephadex LH-20 (Sigma-Aldrich). **Dialysis tubes** with molecular weight cut-off 1 kDa were bought from Spectrum Labs.

Microwave synthesis was performed on a CEM Discover-SP.

NMR spectra were obtained on a Varian Inova spectrometer (500 MHz ^{1}H and 126 MHz ^{13}C) or a Varian 400 MHz NMR spectrometer (400 MHz ^{1}H and 101 MHz ^{13}C). Chemical shifts are reported in ppm using the solvent residual signal as an internal reference (Chloroform-*d*: δ_H = 7.26 ppm, δ_C = 77.23 ppm; Dimethylsulfoxide-d_6: δ_H = 2.50, δ_C = 39.51). The resonance multiplicity is described as s (singlet), d (doublet), t (triplet), …, m (multiplet), br (broad signal).

Photophysical characterization. Absorption spectra of compounds were recorded on air-equilibrated solutions at room temperature with an Agilent Cary 5000 UV-Vis spectrophotometer, using quartz cells with path length of 1.0 cm. Emission spectra were recorded on an Agilent Cary Eclipse fluorescence spectrofluorometer, using quartz cells with path length of 1.0 cm.

Fourier-transform infrared spectra (KBr) were recorded on a Perkin Elmer 2000 spectrometer.

Spectroelectrochemistry was performed using a Metrohm µAutolab III/FRA2 potentiostat and a Carry 5000 spectrometer from Varian, using tetrabutylammonium hexafluorophosphate as a supporting electrolyte.

Ultrafast transient absorption (TA) experiments were conducted using an amplified Ti/sapphire laser system (Clark MXR CPA2101 and 2110, FWHM = 150 fs, λ_{exc} = 387 or 500 nm, 200-300 nJ per pulse) with TA pump / probe Helios detection systems from Ultrafast Systems. White light was generated using a sapphire crystal. Optical densities (OD) of the samples were typically around 0.5 at the excitation wavelengths. A magic angle configuration was employed to avoid rotational dynamics.

Melting points (m.p.) were measured on a Büchi SMP-20 in open capillary tubes and are uncorrected.

IR spectra (KBr) were recorded on a Perkin Elmer 2000 spectrometer.

Chemicals. L-Arginine (Fluorochem, ≥98%), ethylenediamine (Sigma-Aldrich, ≥99.5%), and other reagents and solvents were purchased (Sigma-Aldrich, Fluorochem, TCI Europe, Acros and Alfa Aesar) and used without further purifications. Ultrapure fresh water obtained from a Millipore water purification system (18.2 Milli-Q, Millipore) was used. **Deuterated solvents** from Cambridge Isotope Laboratories and VWR. Generally, dry solvents were purchased and used without further purification.

2. Syntheses

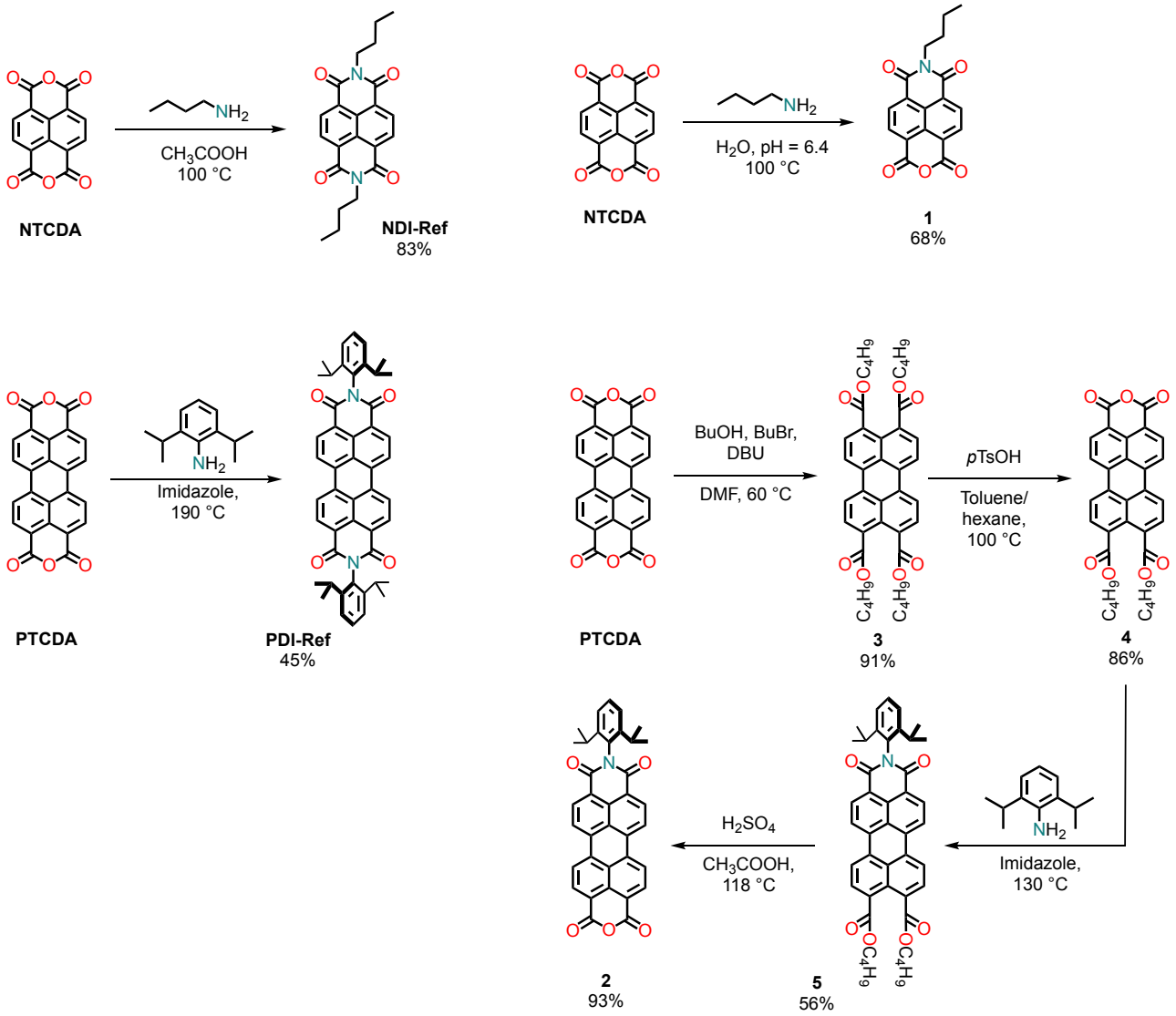

Figure S1. Synthetic scheme for the preparation of the naphthalene and perylene monoimide monoanhydrides, as well as the NDI and PDI reference molecules.

***N,N'*-bis(*n*-butyl)naphthalene-1,4,5,8-tetracarboxylic diimide (NDI-Ref)**

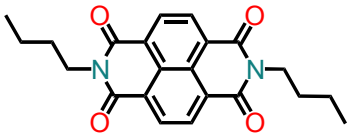

This compound was prepared according to a literature procedure.[1] A suspension of naphthalene-1,4,5,8-tetracarboxylic dianhydride (1.00 g, 3.78 mmol), *n*-butylamine (1.45 mL, 14.92 mmol) in AcOH (22.0 mL) was stirred at 100 °C overnight. After cooling to r.t., the reaction mixture was filtered and washed with MeOH, diethyl ether, and hexane. Purification by column chromatography (SiO_2, 40-63 µm, CH_2Cl_2) gave product **NDI-Ref** as a pale yellow solid (1.19 g, 83% yield).

m.p. 236-238 °C. ^{1}H-NMR (500 MHz, Chloroform-*d*): δ 8.75 (s, 4H), 4.20 (t, *J* = 7.6 Hz, 4H), 1.78 – 1.68 (m, 4H), 1.45 (h, *J* = 7.5 Hz, 4H), 0.99 (t, *J* = 7.7 Hz, 6H). ^{13}C-NMR (126 MHz, Chloroform-*d*): δ 163.07, 131.14, 126.91, 126.86, 40.97, 30.38, 20.55, 14.02. IR (KBr): cm^{-1} 2972, 2939, 2871, 2856, 1701, 1655, 1578, 1460, 1456, 1376, 1345, 1330, 1306, 1286, 1249, 1241, 1222, 1194, 1150, 1077, 981, 944, 893, 858, 773, 742, 718. Characterization in accordance with literature.[1]

***N*-(*n*-butyl)naphthalene-1,4,5,8-tetracarboxylic monoimide monoanhydride (1)**

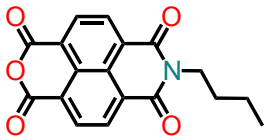

This compound was prepared according to a literature procedure.[2] To a mixture of naphthalene-1,4,5,8-tetracarboxylic dianhydride (0.50 g, 1.86 mmol) in water (175 mL) was added a 1 M aq. KOH solution (17.5 mL). The mixture was vigorously stirred and heated until a clear solution was obtained. At this point, the pH of the solution was acidified to 6.4 by adding 1 M aq. H_3PO_4. After addition of *n*-butylamine (0.20 mL, 2.05 mmol), the pH was readjusted to 6.4 with 1 M aq. H_3PO_4 and the mixture was refluxed overnight. The reaction mixture was then allowed to cool down to r.t. and filtered. After adding CH_3COOH (5 mL) to the filtrate, the off-white solid formed was recovered by filtration and dried under vacuum to afford **NDI 1** (0.40 g, 67% yield).

m.p. >250 °C. ^{1}H-NMR (500 MHz, DMSO-d_6): 8.54 (d, J = 7.5 Hz, 2H), 8.16 (d, J = 7.5 Hz, 2H), 4.05 (t, J = 7.3 Hz 2H), 1.68 – 1.58 (m, 2H), 1.36 (h, J = 7.4 Hz, 2H), 0.93 (t, J = 7.4 Hz, 3H). ^{13}C-NMR (126 MHz, DMSO-d_6): δ 168.54, 162.85, 137.85, 130.05, 128.91, 128.52, 125.49, 124.24, 40.10, 29.54, 19.76, 13.70. IR (KBr): cm^{-1} 2964, 2876, 1707, 1663, 1595, 1471, 1450, 1389, 1357, 1332, 1302, 1246, 1233, 1222, 1087, 968, 887, 768. Characterization in accordance with literature.[2,3]

_N,N_'-bis(2,6-diisopropylphenyl)perylene-3,4,9,10-tetracarboxylic diimide (PDI-Ref)

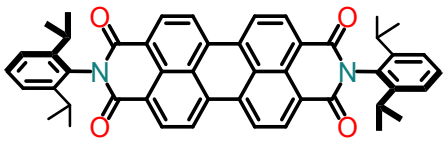

This compound was synthesized according to a literature procedure.[4] A mixture of perylene-3,4,9,10-tetracarboxylic dianhydride (1.00 g, 2.55 mmol), 2,6-diisopropylaniline (2.0 mL, 10.6 mmol) and imidazole (7.5 g) was heated to 190 °C for 24 h, under Ar. The mixture was allowed to cool down to r.t. and diluted with EtOH (50 mL) and 2 M aq. HCl (60 mL) This mixture was stirred for 3 h, then filtered and dried. The mixture was purified by column chromatography (SiO_2, 40-63 µm, CH_2Cl_2) to yield **PDI-Ref** as red solid (0.82 g, 45% yield).

m.p. >250 °C. ^{1}H-NMR (500 MHz, Chloroform-d): δ 8.80 (d, J = 8.0 Hz, 4H), 8.75 (d, J = 8.1 Hz, 4H), 7.51 (t, J = 7.8 Hz, 2H), 7.36 (d, J = 7.8 Hz, 4H), 2.76 (hept, J = 6.7 Hz, 4H), 1.19 (d, 12H), 1.18 (s, J = 6.8 Hz, 24H). ^{13}C-NMR (126 MHz, Chloroform-d): δ 163.44, 145.61, 135.05, 132.07, 130.48, 130.16, 129.71, 129.65, 126.83, 124.10, 123.40, 123.30, 29.22, 23.97. IR (KBr): cm^{-1} 2961, 2929, 2868, 1705, 1666, 1593, 1579, 1467, 1453, 1429, 1403, 1383, 1356, 1346, 1252, 1199, 1178, 1126, 958, 834, 815, 797, 750, 742. Characterization in accordance with literature.[4]

Perylene-3,4,9,10-tetracarboxylic tetrabutylester (3)

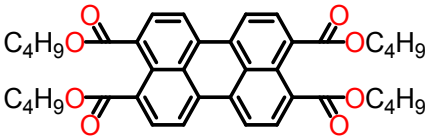

This compound was synthesized according to a literature procedure.[5] Perylene-3,4,9,10-tetracarboxylic dianhydride (3.9 g, 10.0 mmol), 1,5-diazabiciclo(5.4.0)undec-7-ene (6.0 mL, 40.0 mmol) and *n*-butanol (7.3 mL, 80.0 mmol) were dissolved in DMF (50 mL) and stirred at 60 °C for 30 min. Then, a solution of 1-bromobutane (8.6 mL, 80.0 mmol) in DMF (30 mL) were added and the mixture was stirred overnight at 60 °C. The mixture was allowed to cool down to r.t. and was poured into H_2O (400 mL) and left stirring for 15 min. The precipitate was filtered, washed with H_2O and dried under vacuum. Purification by column chromatography (SiO_2, 40-63 µm, CHX/CH_2Cl_2 1:1) afforded product **3** as bright yellow solid (5.94 g, 91% yield).

m.p. 166-242 °C. ^{1}H-NMR (400 MHz, Chloroform-*d*): 8.11 (d, J = 7.7 Hz, 4H), 7.94 (d, *J* = 7.9 Hz, 4H), 4.35 (t, *J* = 6.8 Hz, 8H), 1.89 – 1.71 (m, 8H), 1.55 – 1.45 (m, 8H), 1.01 (t, *J* = 7.4 Hz, 12H). ^{13}C-NMR (101 MHz, Chloroform-*d*): δ 168.67, 132.99, 130.49, 130.46, 128.99, 128.81, 121.44, 65.47, 30.81, 19.43, 13.97. IR (KBr): cm^{-1} 2960, 2935, 2869, 1724, 1707, 1590, 1514, 1475, 1410, 1393, 1377, 1332, 1324, 1308, 1278, 1186, 1172, 1135, 1097, 1067, 1036, 1005, 982, 963, 941, 844, 806, 748. Characterization in accordance with literature.[5,6]

Perylene-3,4,9,10-tetracarboxylic monoanhydride dibutylester (**4**)

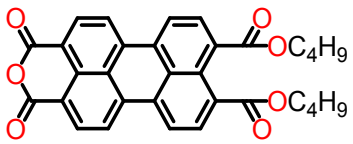

Compound was synthesized according to a modified literature procedure.[7] Perylene-3,4,9,10-tetracarboxylic tetrabutylester **3** (2.0 g, 3.1 mmol) and *p*-toluenesulfonic acid monohydrate (0.6 g, 3.1 mmol) were suspended in a mixture of toluene/hexane (18 mL, 5:1 *v*/*v*) and heated to 100 °C for 5 h. The mixture was left to cool down to r.t., then the solid was filtered, washed with boiling hexane (3×) and acetonitrile (3×). Finally, the solid was dried under vacuum to obtain product **4** as bright red solid (1.40 g, 86% yield).

m.p. >250 °C. ^{1}H-NMR (500 MHz, Chloroform-*d*): δ 8.65 (d, *J* = 7.9 Hz, 2H), 8.53 (d, *J* = 8.3 Hz, 2H), 8.51 (d, *J* = 7.8 Hz, 2H), 8.14 (d, *J* = 7.8 Hz, 2H), 4.36 (t, *J* = 6.8 Hz, 4H), 1.83-1.77 (m, 4H), 1.52-1.48 (m, 4H), 1.00 (t, *J* = 7.4 Hz, 6H). ^{13}C NMR (126 MHz, Chloroform-*d*): δ

168.29, 160.52, 137.53, 133.83, 133.01, 131.79, 130.63, 129.50, 126.64, 123.71, 122.37, 118.24, 65.94, 30.82, 19.47, 14.00. IR (KBr): cm^{-1} 2959, 2933, 2872, 1773, 1729, 1709, 1641, 1594, 1509, 1412, 1384, 1341, 1324, 1286, 1258, 1236, 1203, 1173, 1150, 1126, 1105, 1065, 1016, 860, 807, 751, 736. Characterization in accordance with literature.[8]

***N*-(2,6-diisopropylphenyl)perylene-3,4,9,10-tetracarboxylic monoimide dibutylester (5)**

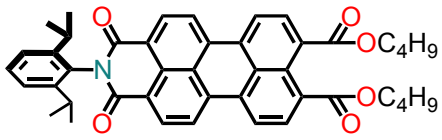

Compound was synthesized according to a modified literature procedure.[9] A mixture of perylene-3,4,9,10-tetracarboxylic monoanhydride dibutylester **4** (0.50 g, 0.96 mmol) and imidazole (3.00 g) was heated to 110 °C, under Ar. Then, 2,6-diisopropylaniline (0.31 mL, 1.65 mmol) was added dropwise and the reaction mixture was heated to 130 °C and stirred for 5 h. After cooling to 110 °C, the dark red solution was quenched with H_2O (5 mL) and stirred for 10 min. Next, the mixture was poured into H_2O (20 mL) and stirred for 2 h. The red solid was recovered by filtration and dried under vacuum. Purification by column chromatography (SiO_2, 40-63 µm, CH_2Cl_2) afforded product **5** as bright red solid (0.37 g, 56% yield).

m.p. >250 °C. ^{1}H NMR (400 MHz, Chloroform-*d*): δ 8.70 (d, *J* = 8.0 Hz, 2H), 8.55 (d, *J* = 8.1 Hz, 2H), 8.52 (d, *J* = 8.0 Hz, 2H), 8.14 (d, *J* = 7.9 Hz, 2H), 7.49 (*t*, *J* = 7.8 Hz, 1H), 7.34 (d, *J* = 7.7 Hz, 2H), 4.36 (t, *J* = 6.8 Hz, 4H), 2.75 (hept, *J* = 6.8 Hz, 2H), 1.89 – 1.70 (m, 4H), 1.54 – 1.42 (m, 4H), 1.18 (d, *J* = 6.9 Hz, 12H), 1.00 (t, *J* = 7.4 Hz, 6H). ^{13}C-NMR (101 MHz, Chloroform-*d*): δ 168.51, 168.49, 163.92, 145.89, 136.17, 132.39, 132.26, 132.22, 130.97, 130.62, 130.24, 129.79, 129.47, 129.39, 126.59, 124.28, 123.00, 122.39, 122.16, 65.83, 30.84, 29.41, 24.21, 19.48, 14.02. IR (KBr): cm^{-1} 2961, 2931, 2871, 1730, 1707, 1667, 1594, 1508, 1462, 1415, 1384, 1358, 1296, 1264, 1249, 1199, 1174, 1162, 1128, 1099, 1065, 954, 938, 849, 824, 806, 749.

***N*-(2,6-diisopropylphenyl)perylene-3,4,9,10-tetracarboxylic monoimide monoanhydride (2)**

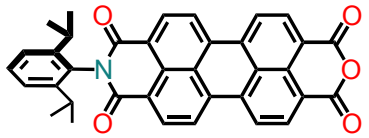

Compound was synthesized according to a modified literature procedure.[10] Perylene-3,4,9,10-tetracarboxylic monoimide diester **5** (0.20 g, 0.29 mmol) was suspended in a mixture of CH_3COOH/H_2SO_4 (15 mL, 20:1 *v*/*v*) and refluxed for 2 h. The mixture was allowed to cool down to r.t. and then poured into H_2O (20 mL). The precipitate was filtered, washed with H_2O, CH_3OH and dried under vacuum to obtain product **2** as dark red solid (0.15 g, 93% yield).

m.p. >250 °C. ^{1}H-NMR (500 MHz, Methylene Chloride-d_2): δ 8.84 – 8.69 (m, 8H), 7.55 (t, J = 7.8 Hz, 1H), 7.39 (d, J = 7.8 Hz, 2H), 2.77 (hept, J = 6.8 Hz, 2H), 1.17 (d, J = 6.8 Hz, 12H). ^{13}C-NMR was not recorded due to the low solubility of the product in most organic solvents. IR (KBr): cm^{-1} 2966, 2928, 2867, 1772, 1734, 1702, 1662, 1596, 1579, 1506, 1461, 1405, 1365, 1322, 1249, 1183, 1152, 1124, 1021, 855, 843, 811, 761, 747, 740.

Nitrogen-doped Carbon Nanodots (**NCNDs**). NCNDs were obtained following our synthetic procedure.[11,12] In a typical scale-up reaction, consecutively 8 microwave vials containing aqueous solution of L-Arginine (L-Arg, 87.0 mg) and ethylenediamine (EDA, 33.0 µL) in Milli-Q water (100.0 µL) were heated via microwave at 240 °C, 26 bar and 200 W for 180 seconds. The solutions were diluted with water, were filtered through a 0.1 µm filter membrane (Millipore; Merck, cat. no. JVWP02500) and the filtrate was dialyzed against pure water through a dialysis membrane for 48 h. Typically, 8 reaction mixtures require (concurrent) dialyses in 4 separate 2 L beakers (each containing 10 mL of reaction mixture). The aqueous solution of NCNDs was then lyophilized giving a yellowish solid (NCNDs: 176.0 mg).

Synthesis of hybrids – typical procedure. A suspension of NCNDs (50.0 mg, *ca.* 1350 µmol g^{-1} amines) and the appropriate monoimide monoanhydride precursor (0.25 eq. based on Kaiser Test, 4.80 mg or 10.55 mg for **1** and **2**, respectively), dry triethylamine (90 µL) and

dry DMF (2.5 mL) were heated to 140 °C for 30 minutes, under microwave irradiation. After completion of the reaction, the reaction mixture was loaded directly into a SEC column (Sephadex™ LH-20, DMF as mobile phase). The fractions were followed by either using UV lamp or tracking the colored material, which was collected into test tubes. Before combing the fractions, they were checked by UV-Vis spectroscopy. The collected material was then concentrated under reduced pressure (with the aid of toluene), re-dissolved in water and finally lyophilized to obtain the product as powder. In a typical synthesis of NDI and PDI hybrid, we used NCND (50.0 mg), **1** (4.90 mg, 0.25 eq.) and **2** (10.55 mg, 0.25 eq), dry triethylamine (90 µL) and dry DMF (2.5 mL) were heated to 140 °C for 30 minutes, under microwave irradiation. The work-up was the same as described above.

3. Infrared Spectrophotometry

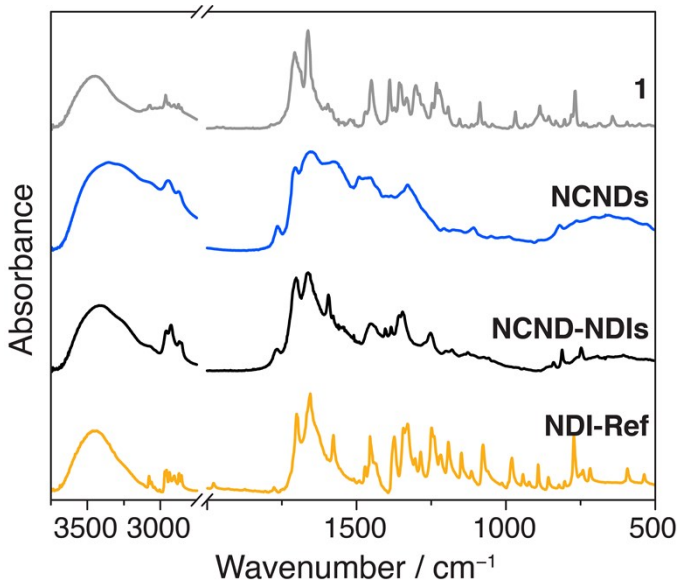

Figure S2. FT-IR absorption spectra for precursor 1 (gray trace), NCNDs (blue trace), NCND-NDIs (black trace) and NDI-Ref (orange trace).

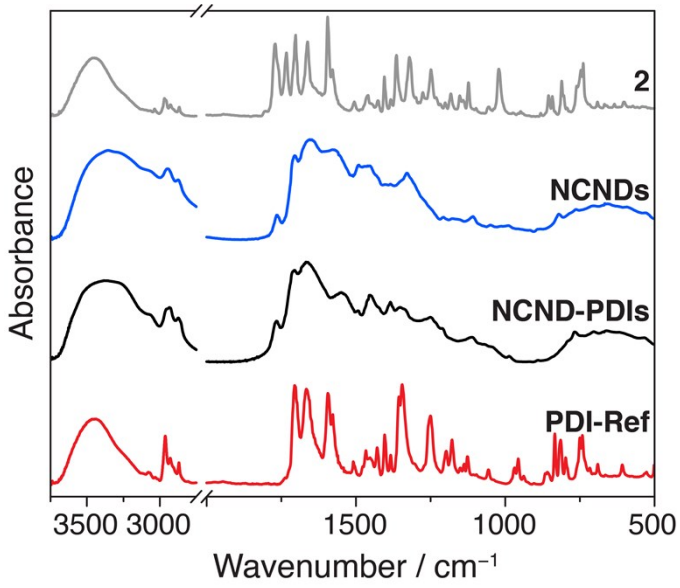

Figure S3. FT-IR absorption spectra for precursor 2 (gray trace), NCNDs (blue trace), NCND-PDIs (black trace) and PDI-Ref (red trace).

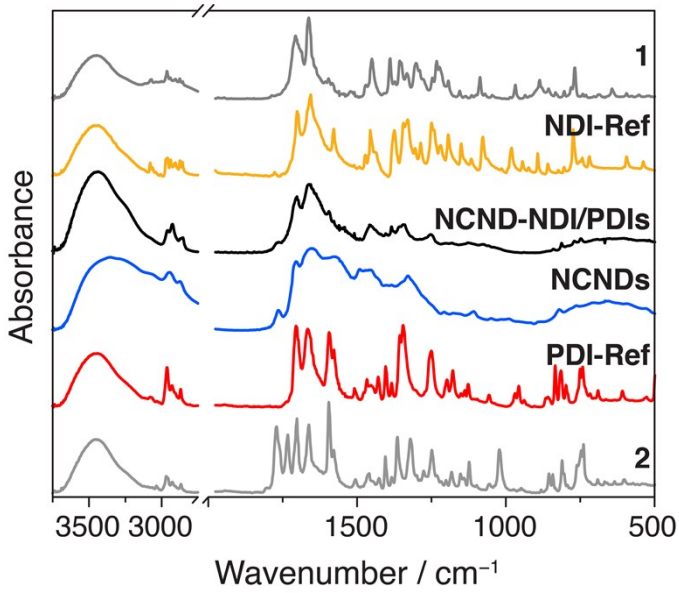

Figure S4. FT-IR absorption spectra for precursor 1 (gray trace), NDI-Ref (orange trace), NCND-NDI/PDIs (black trace), NCNDs (blue trace), PDI-Ref (red trace) and 2 (gray trace).

4. Photophysical Measurements

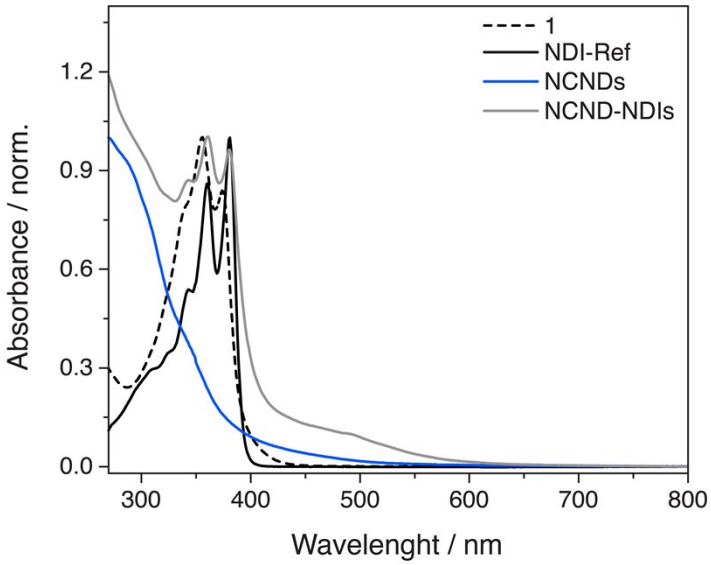

Figure S5. UV-Vis absorption spectra in DMF for precursor 1 (black dashed trace), NDI-Ref (black trace), NCNDs (blue trace) and NCND-NDIs (gray trace).

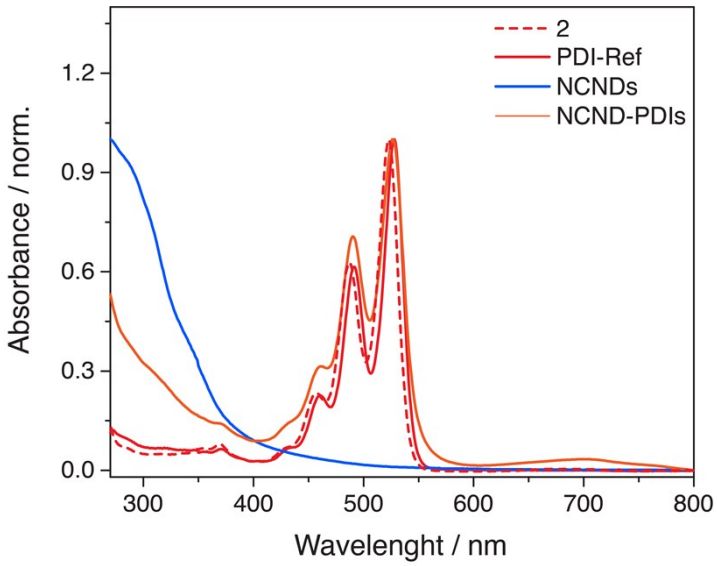

Figure S6. UV-Vis absorption spectra in DMF for precursor 2 (red dashed trace), PDI-Ref (red trace), NCNDs (blue trace) and NCND-PDIs (orange trace).

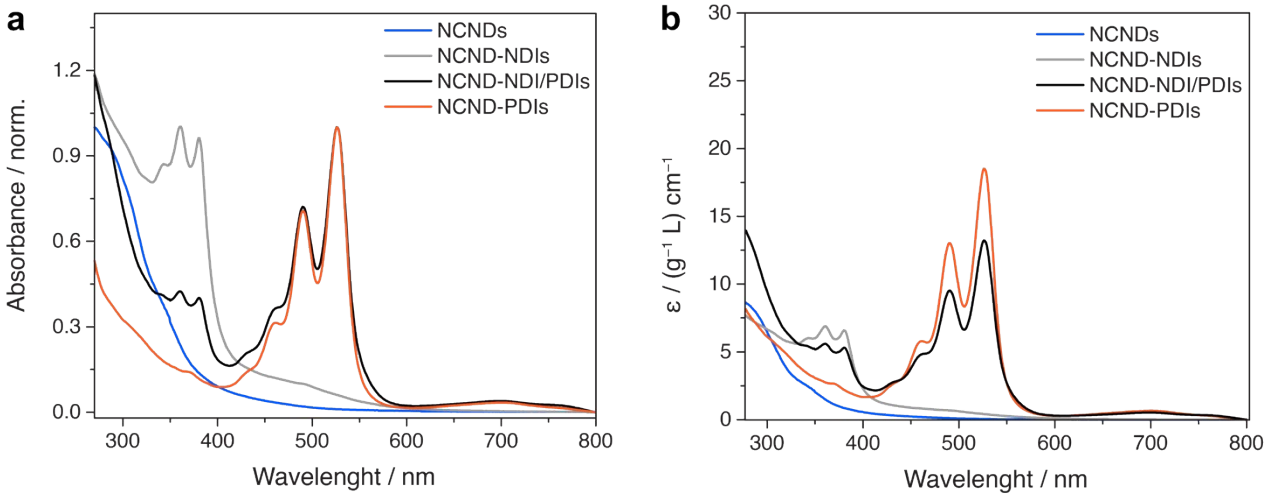

Figure S7. UV-Vis absorption as a) normalized spectra and as b) mass extinction coefficient in DMF for NCNDs (blue trace), NCND-NDIs (gray trace), NCND-NDI/PDIs (black trace), and NCND-PDIs (orange trace).

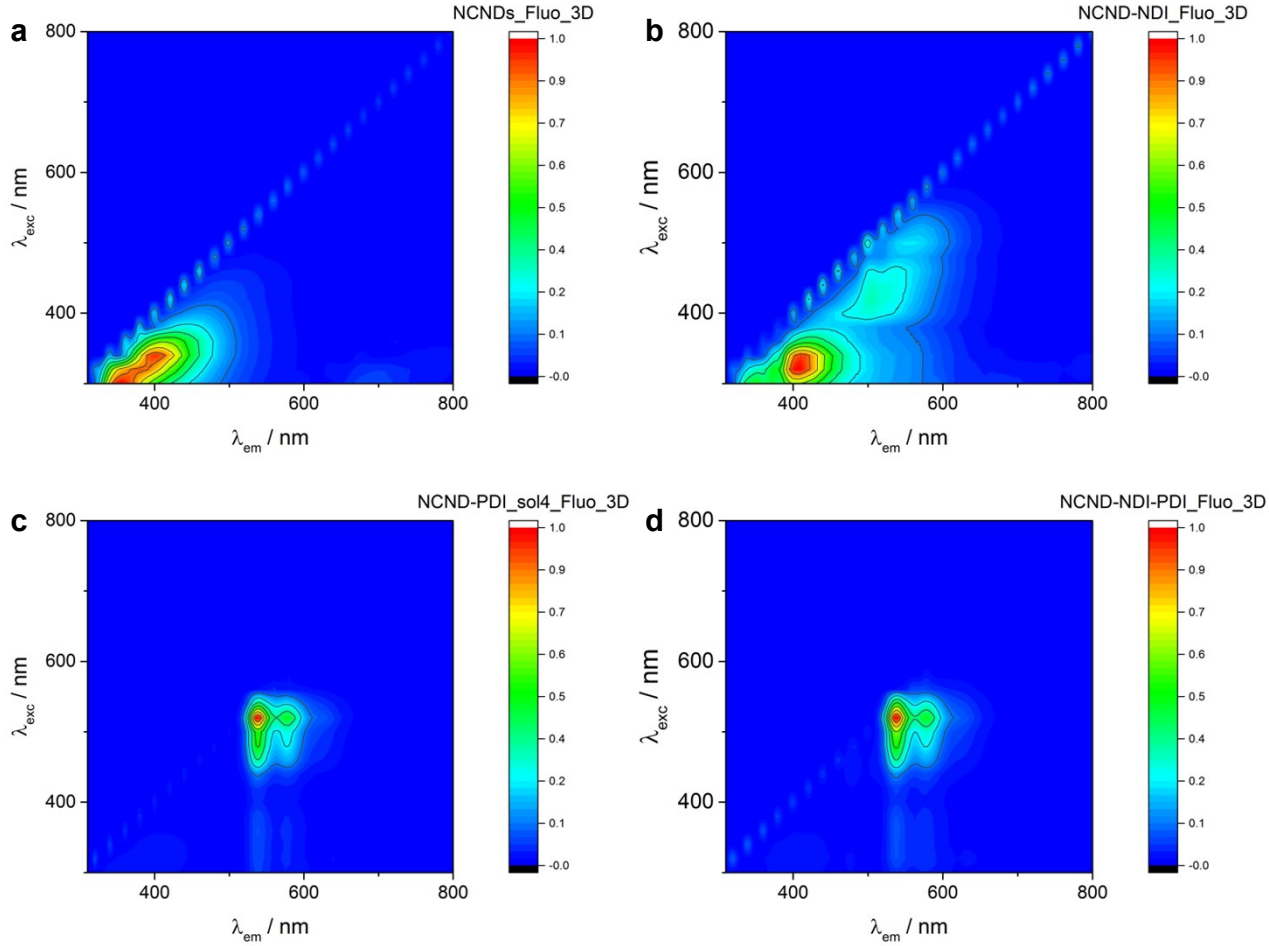

Figure S8. Fluorescence emission-excitation matrix for (**a**) NCNDs, (**b**) NCND-NDIs, (**c**) NCND-PDIs and (**d**) NCND-NDI/PDIs.

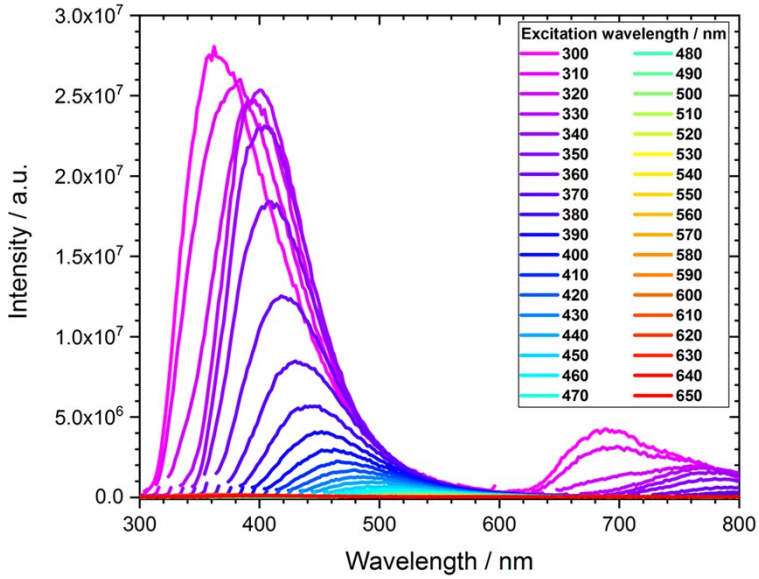

Figure S9. Fluorescence emission at different excitation wavelengths for NCNDs.

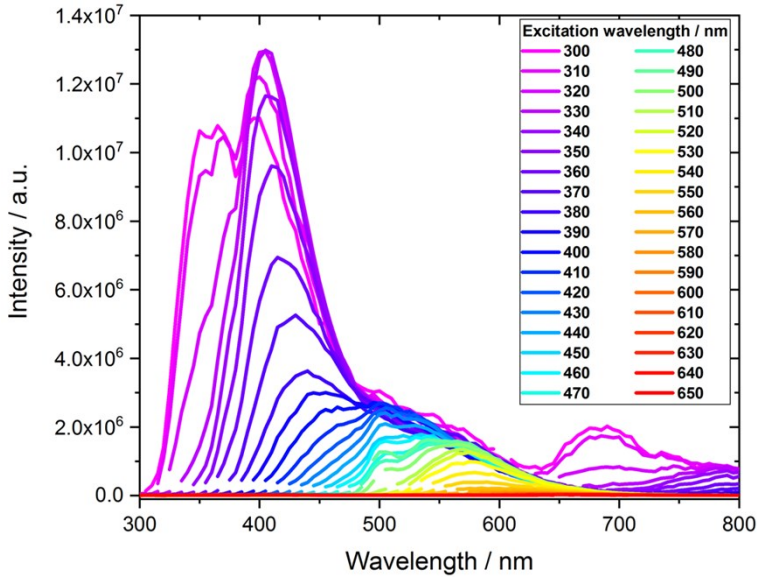

Figure S10. Fluorescence emission at different excitation wavelengths for NCND-NDI.

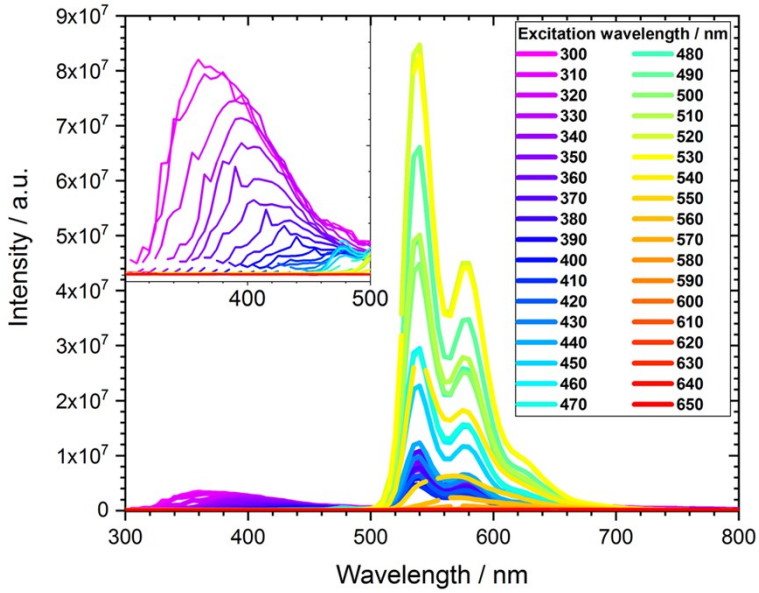

Figure S11. Fluorescence emission at different excitation wavelengths for NCND-PDI.

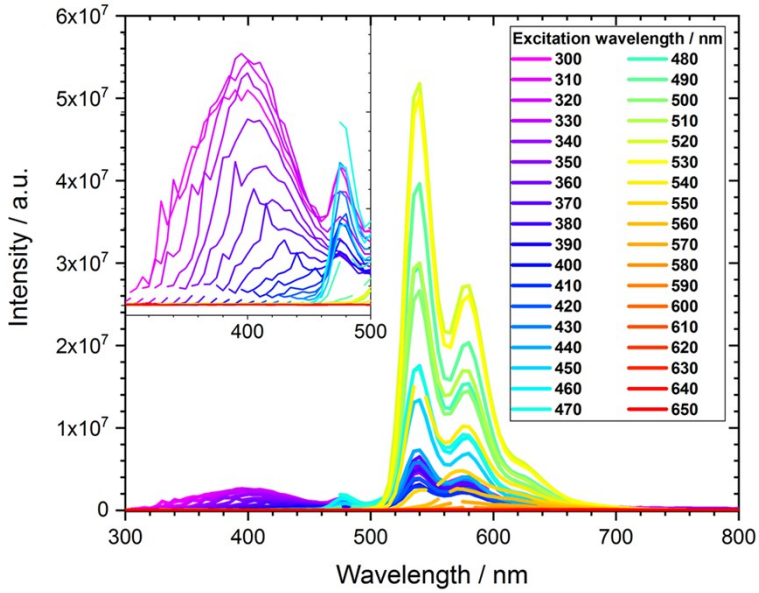

Figure S12. Fluorescence emission at different excitation wavelengths for NCND-NDI/PDI.

5. Spectroelectrochemistry

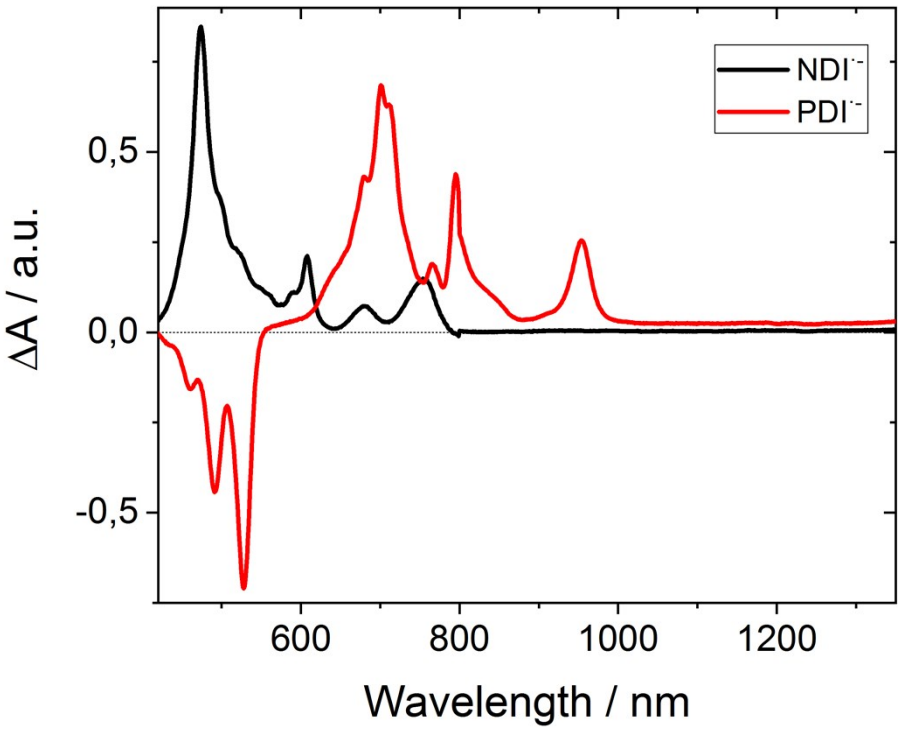

Figure S13. Spectroelectrochemical differential absorption spectra upon reduction of NDI-Ref (black curve) and PDI-Ref (red curve) in DMF, at −0.3 V and −0.4V, respectively.

6. Transient Absorption Spectroscopy

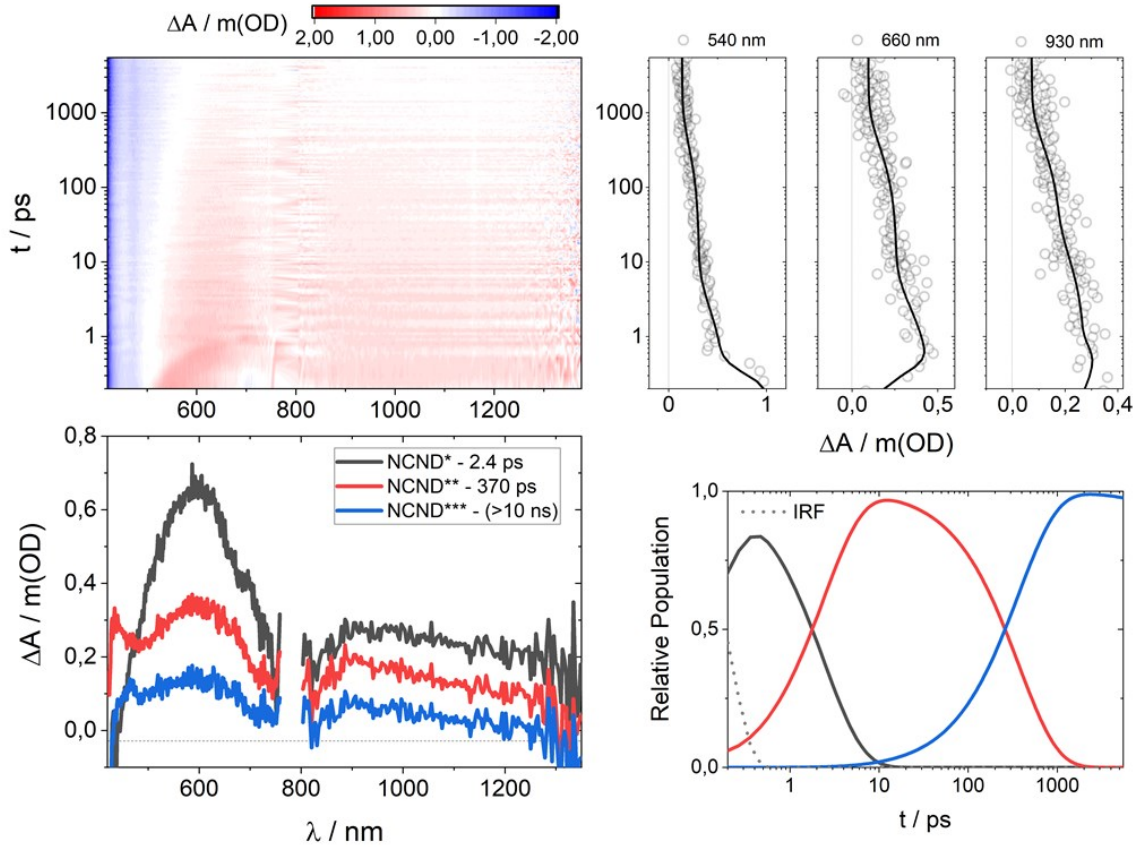

Figure S14. Top left: Differential absorption 3D map obtained upon fs-TAS on NCNDs, in DMF at room temperature, with 387 nm excitation. Top right: Time absorption profiles and corresponding fittings at 540, 660 and 930 nm. Bottom left: Species associated differential spectra of the NCND* (black), NCND** (red) and NCND*** (blue) excited states. Bottom right: concentration evolution over time.

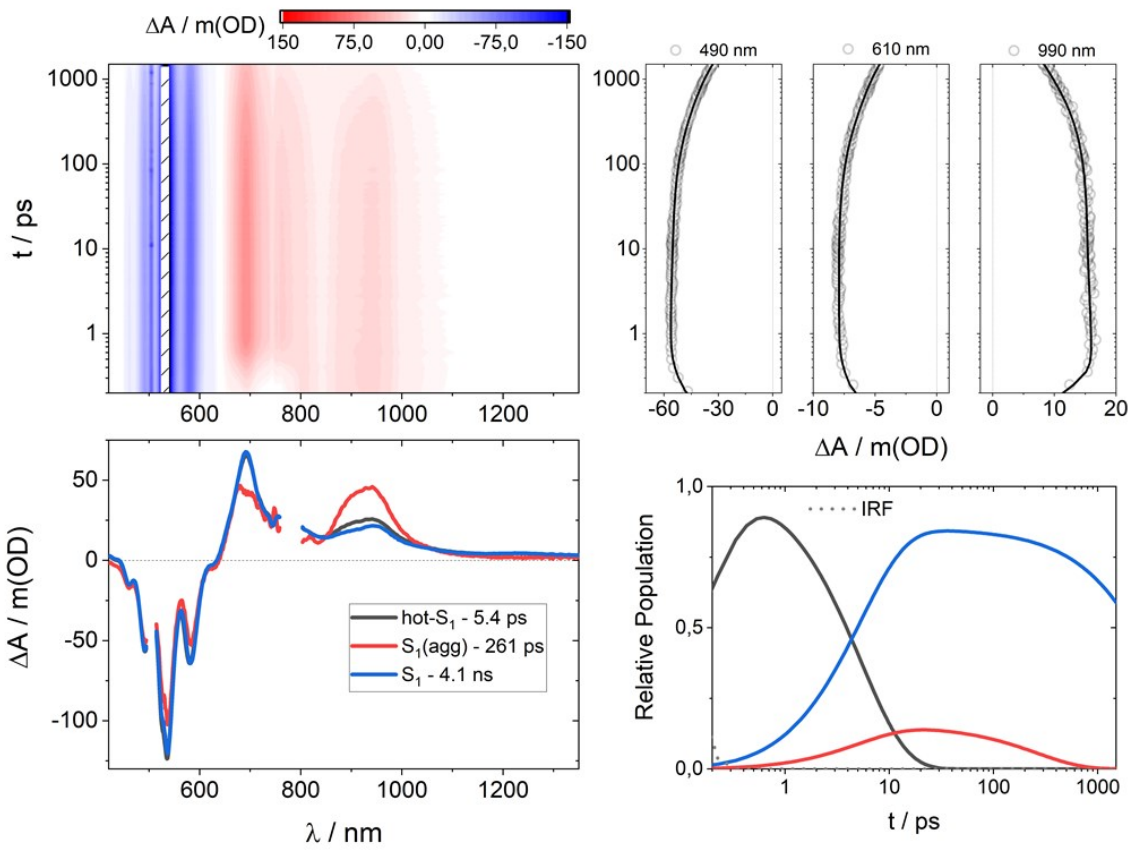

Figure S15. Top left: Differential absorption 3D map obtained upon fs-TAS on PDI-Ref, in DMF at room temperature, with 500 nm excitation. Top right: Time absorption profiles and corresponding fittings at 490, 610 and 990 nm. Bottom left: Species associated differential spectra of the hot-S_1 (black), S_1(agg) (red) and S_1 (blue) excited states. Bottom right: concentration evolution over time.

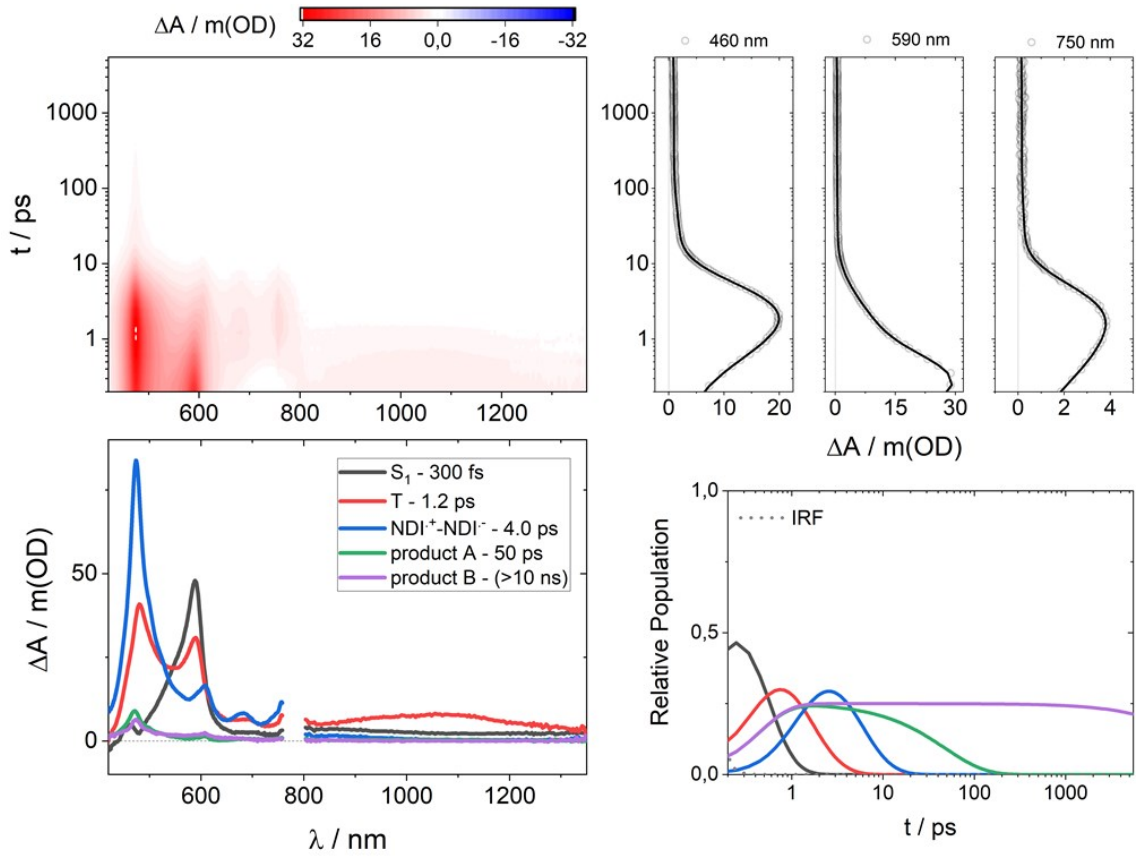

Figure S16. Top left: Differential absorption 3D map obtained upon fs-TAS on NDI-Ref, in DMF at room temperature, with 387 nm excitation. Top right: Time absorption profiles and corresponding fittings at 460, 590 and 750 nm. Bottom left: Species associated differential spectra of the S_1 (black), T (red), $NDI^{\cdot+}$-$NDI^{\cdot-}$ (blue) product A (green) and product B (purple) excited states. Bottom right: concentration evolution over time.

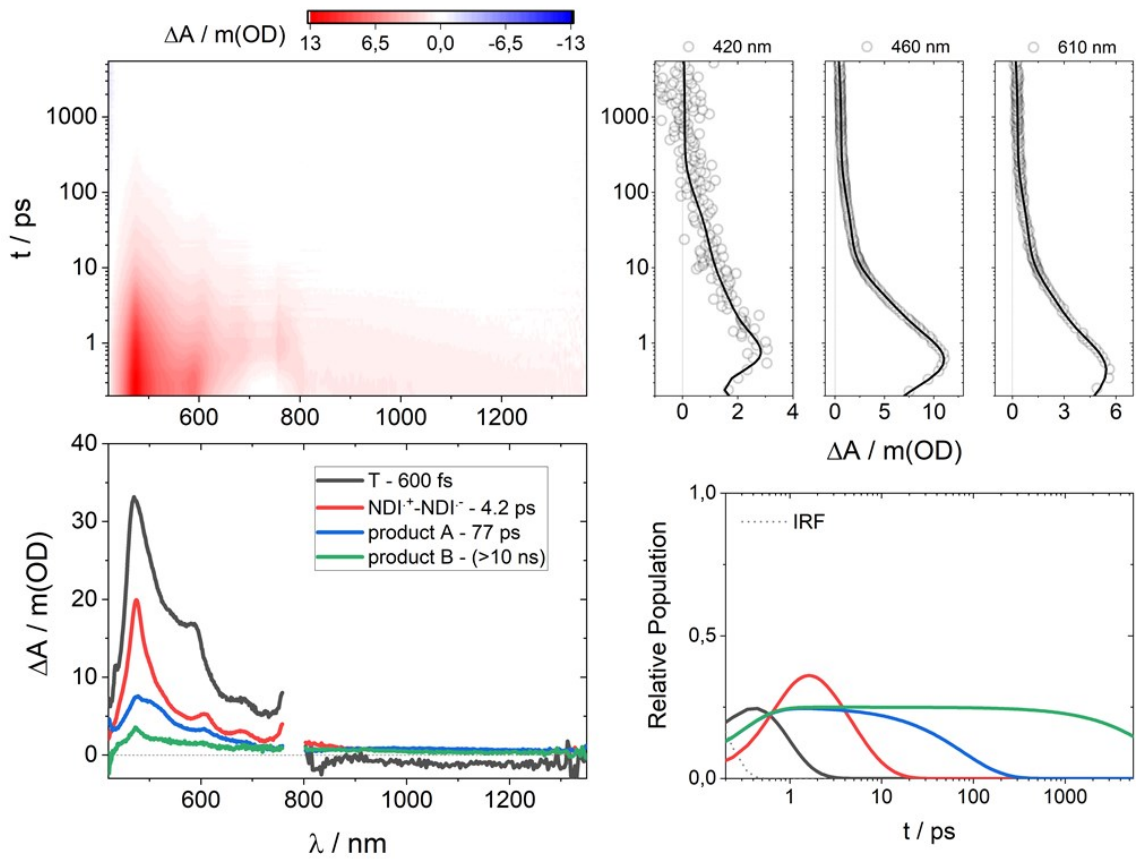

Figure S17. Top left: Differential absorption 3D map obtained upon fs-TAS on NCND-NDIs, in DMF at room temperature, with 387 nm excitation. Top right: Time absorption profiles and corresponding fittings at 420, 460 and 610 nm. Bottom left: Species associated differential spectra of the T (black), $NDI^{\bullet+}$-$NDI^{\bullet-}$ (red), product A (blue) and product B (green) excited states. Bottom right: concentration evolution over time.

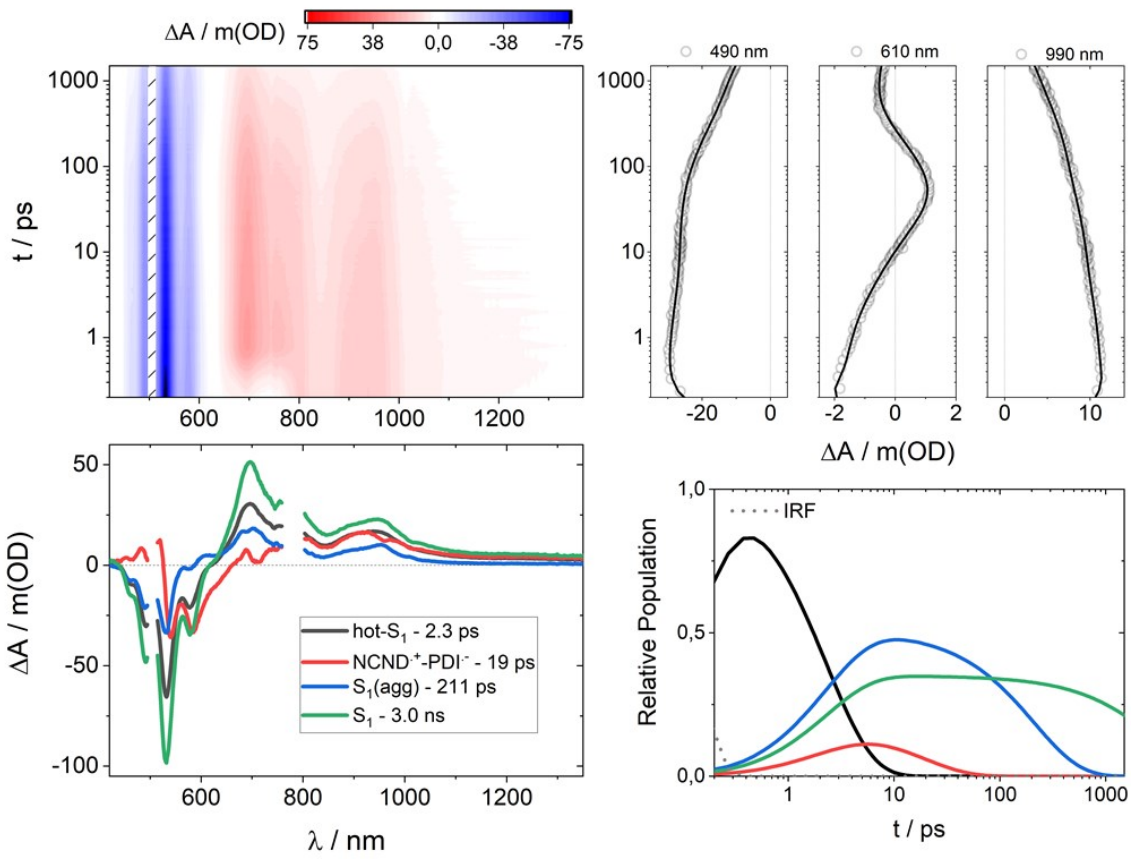

Figure S18. Top left: Differential absorption 3D map obtained upon fs-TAS on NCND-PDIs, in DMF at room temperature, with 500 nm excitation. Top right: Time absorption profiles and corresponding fittings at 490, 610 and 990 nm. Bottom left: Species associated differential spectra of the hot-S_1 (black), $NCND^{\cdot+}$-$PDI^{\cdot-}$ (red), S_1(agg) (blue) and S_1 (green) excited states. Bottom right: concentration evolution over time.

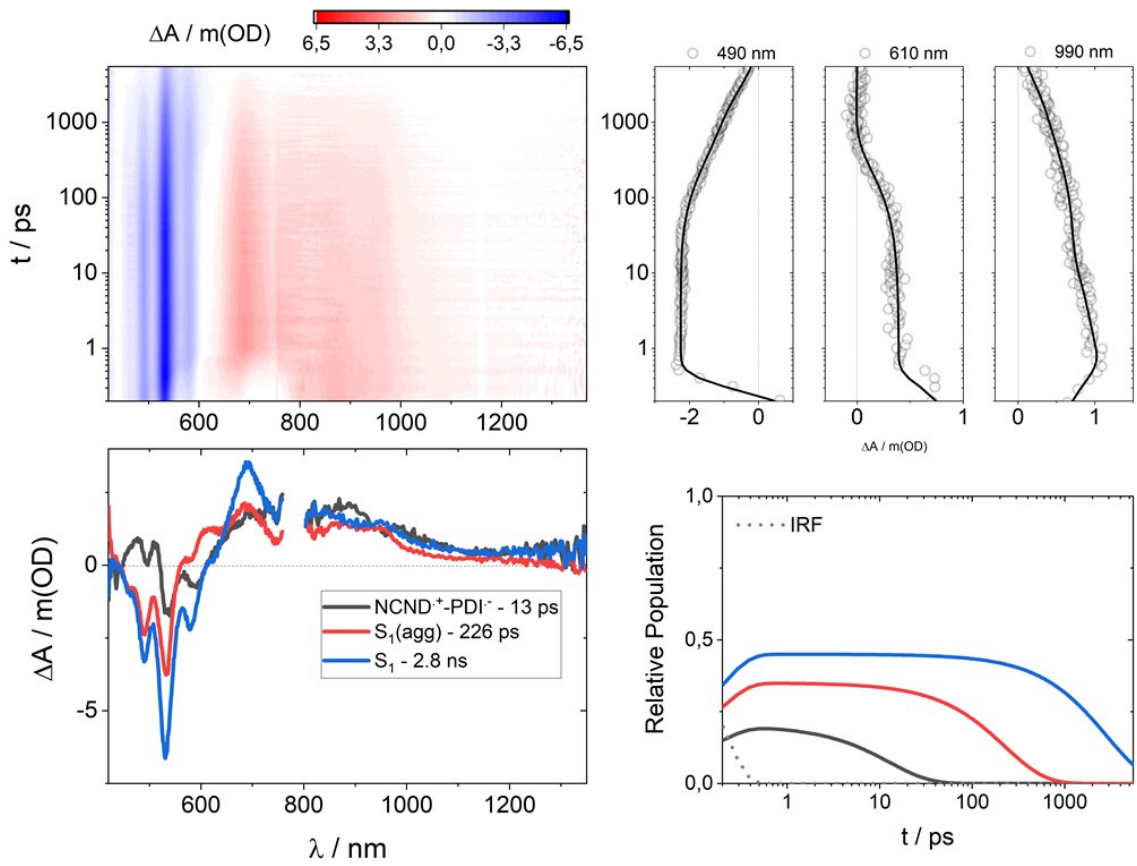

Figure S19. Top left: Differential absorption 3D map obtained upon fs-TAS on NCND-PDIs, in DMF at room temperature, with 387 nm excitation. Top right: Time absorption profiles and corresponding fittings at 490, 610 and 990 nm. Bottom left: Species associated differential spectra of the $NCND^{\cdot+}$-$PDI^{\cdot-}$ (black), S_1(agg) (red), and S_1 (blue) excited states. Bottom right: concentration evolution over time.

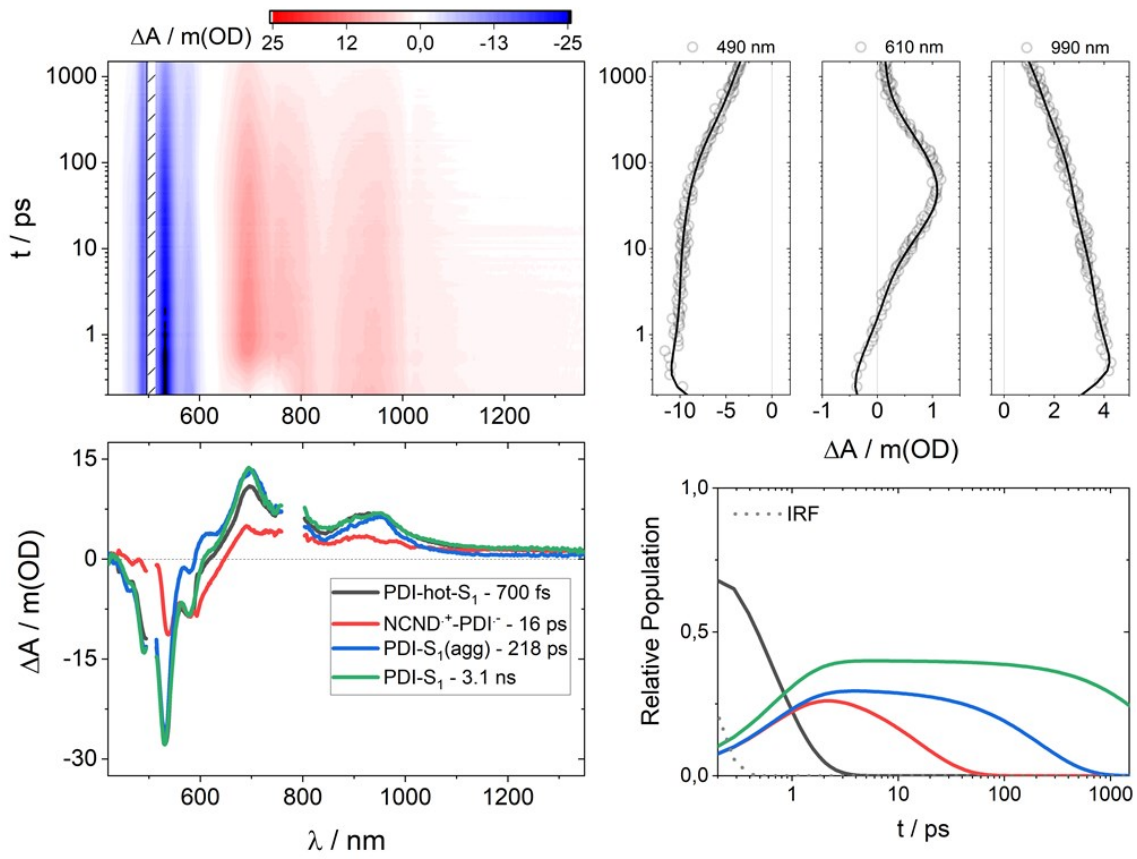

Figure S20. Top left: Differential absorption 3D map obtained upon fs-TAS on NCND-NDI/PDIs, in DMF at room temperature, with 500 nm excitation. Top right: Time absorption profiles and corresponding fittings at 490, 610 and 990 nm. Bottom left: Species associated differential spectra of the PDI centered hot-S_1 (black), $NCND^{\cdot+}$-$PDI^{\cdot-}$ (red), PDI-centered S_1(agg) (blue) and PDI-centered S_1 (green) excited states. Bottom right: concentration evolution over time.

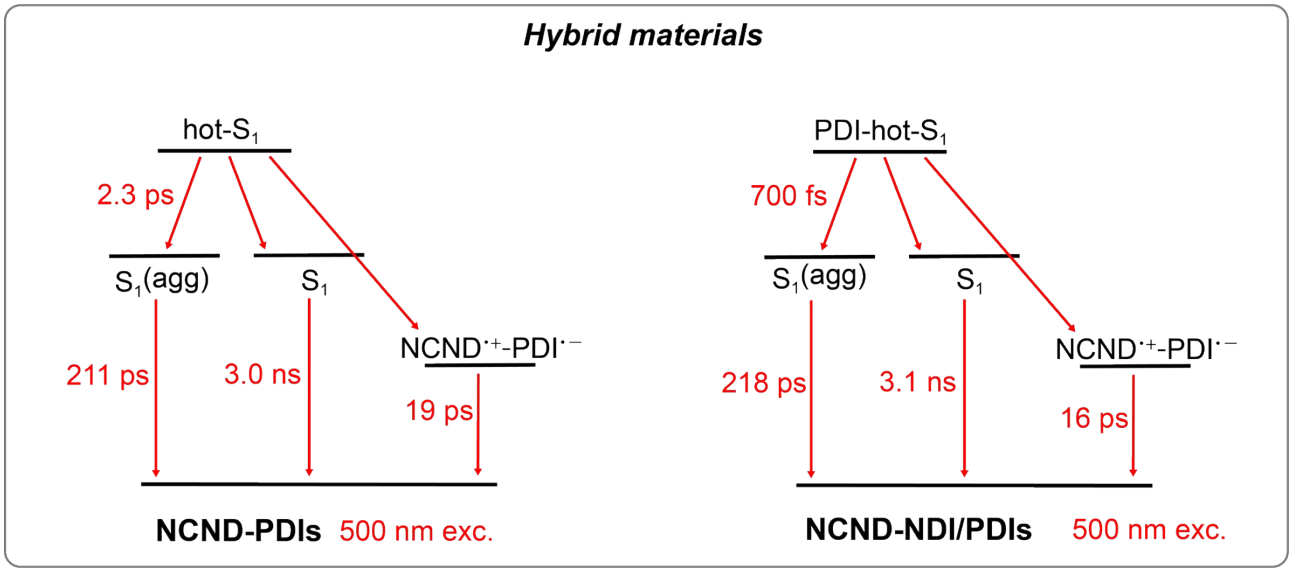

Figure S21. Kinetic models used to fit the fs-TAS data of hybrid materials (NCND-PDIs, NCND-NDI/PDIs) under 500 nm excitation.

7. References

[1] Y. Matsunaga, K. Goto, K. Kubono, K. Sako, T. Shinmyozu, *Chem. - A Eur. J.* **2014**, *20*, 7309–7316.

[2] S. K. M. Nalluri, C. Berdugo, N. Javid, P. W. J. M. Frederix, R. V. Ulijn, *Angew. Chem. Int. Ed.* **2014**, *53*, 5882–5887.

[3] H. Shao, T. Nguyen, N. C. Romano, D. A. Modarelli, J. R. Parquette, *J. Am. Chem. Soc.* **2009**, *131*, 16374–16376.

[4] C. Ramanan, A. L. Smeigh, J. E. Anthony, T. J. Marks, M. R. Wasielewski, *J. Am. Chem. Soc.* **2011**, *134*, 386–397.

[5] Y. Li, C. Wang, C. Li, S. Di Motta, F. Negri, Z. Wang, *Org. Lett.* **2012**, *14*, 5278–5281.

[6] X. Mo, M. M. Shi, J. C. Huang, M. Wang, H. Z. Chen, *Dye. Pigment.* **2008**, *76*, 236–242.

[7] L. George, Z. Ahmed, H. Lemmetyinen, A. Efimov, *European J. Org. Chem.* **2015**, *2015*, 584–590.

[8] J. E. A. Webb, K. Chen, S. K. K. Prasad, J. P. Wojciechowski, A. Falber, P. Thordarson, J. M. Hodgkiss, *Phys. Chem. Chem. Phys.* **2016**, *18*, 1712–1719.

[9] W. E. Benjamin, D. R. Veit, M. J. Perkins, E. Bain, K. Scharnhorst, S. McDowall, D. L. Patrick, J. D. Gilbertson, *Chem. Mater.* **2014**, *26*, 1291–1293.

[10] V. Kunz, V. Stepanenko, F. Würthner, *Chem. Commun.* **2015**, *51*, 290–293.

[11] F. Arcudi, L. Đorđević, M. Prato, *Angew. Chem. Int. Ed.* **2016**, *55*, 2107–2112.

[12] L. Đorđević, F. Arcudi, M. Prato, *Nat. Protoc.* **2019**, *14*, 2931–2953.